European Journal of Pharmaceutics and Biopharmaceutics 76 (2010) 24–37

Contents lists available at ScienceDirect

European Journal of Pharmaceutics and Biopharmaceutics

journal homepage: www.elsevier.com/locate/ejpb

Research paper

N-alkylation of poloxamines modulates micellar assembly and encapsulation and release of the antiretroviral efavirenz

Diego A. Chiappetta [a,b], Carmen Alvarez-Lorenzo [c], Ana Rey-Rico [c], Pablo Taboada [d], Angel Concheiro [c], Alejandro Sosnik [a,b,*]

[a] *Department of Pharmaceutical Technology, University of Buenos Aires, Buenos Aires, Argentina*
[b] *National Science Research Council (CONICET), Buenos Aires, Argentina*
[c] *Departamento de Farmacia y Tecnología Farmacéutica, Universidad de Santiago de Compostela, Santiago de Compostela, Spain*
[d] *Departamento de Física de la Materia Condensada, Universidad de Santiago de Compostela, Santiago de Compostela, Spain*

ARTICLE INFO

Article history:
Received 1 March 2010
Accepted in revised form 16 May 2010
Available online 21 May 2010

Keywords:
Polymeric micelles
Pristine and *N*-alkylated poloxamines self-assembly
HIV/AIDS
Efavirenz encapsulation
Drug release

ABSTRACT

Poloxamines (X-shaped poly(ethylene oxide)–poly(propylene oxide) (PEO–PPO) diblocks connected to a central ethylenediamine group) were *N*-methylated and *N*-allylated with the aim of widening their versatility as drug nanocarriers. The self-aggregation properties of various derivatives, covering a wide range of molecular weights and EO/PO ratios, were thoroughly investigated. The cytocompatibility of different modified poloxamines was compared to that of the pristine counterparts by MTT and LDH assays. The most hydrophilic varieties were highly cytocompatible even at concentrations of 5%. Toward the optimization of the oral pharmacotherapy of the Human Immunodeficiency Virus (HIV) infection in pediatric patients, the encapsulation and *in vitro* delivery of efavirenz (EFV), a lipophilic first-line antiretroviral drug, were evaluated. Pristine and *N*-alkylated poloxamines behaved as highly efficient EFV solubilizers enhancing the aqueous solubility of the drug between 166 and 7426-times. EFV promotes self-micellization of poloxamines; their tiny structural modification (i.e., just one methyl- or allyl-group) being able to regulate drug/micellar core interaction. Despite the physical stability of the micelles against dilution in physiological mimicking fluids, the *N*-alkylated derivatives were slightly more prone to disassembly promoting EFV release from the micellar reservoir. For all the derivatives evaluated, the *in vitro* release fitted zero-order kinetics and was sustained for at least 24 h. These findings point out *N*-alkylated poloxamines as promising nanocarriers for oral or parenteral drug delivery.

1. Introduction

Encapsulation of poorly water-soluble drugs within the hydrophobic core of polymeric micelles represents one of the most attractive nanotechnological strategies to improve their aqueous solubility [1]. The temperature-sensitive poly(ethylene oxide)–poly(propylene oxide) (PEO–PPO) block copolymers have been extensively explored as components of polymeric micelles [2]. Two families are commercially available: (i) the linear PEO–PPO–PEO poloxamers (Pluronic®) and (ii) the branched poloxamines (Tetronic®) (Scheme 1A). Due to the commercial availability of a broader spectrum of molecular weights and EO/PO relative compositions, most of the research has been focused on the former. On the other hand, poloxamines present a central ethylenediamine group that confers the amphiphile dual responsiveness to temperature and pH [3]. This feature enables the fine tuning of the self-aggregation profile and the drug/core interaction by means of the pH of the medium; poloxamine pK_a values are between 4.0 and 5.6 for the first tertiary amine moiety and in the 6.2–8.1 range for the second one [4]. Thus, at pH ~ 2, poloxamines are diprotonated and electrostatic repulsion hinders the self-aggregation and the critical micellar concentration (CMC) is maximal. At pH ~ 7.4, poloxamines become monoprotonated and the aggregation tendency rises (lower CMC), being even higher under basic pH conditions (pH > 8). Due to this unique behavior, poloxamines have attracted much attention during recent years in the context of drug encapsulation and delivery; successful results with simvastatin [4], griseofulvin [5], triclosan [6], triclocarban [7] have been reported. Poloxamines have been also recently investigated *in vivo* as vectors for the transfection of plasmid DNA in cardiac and skeletal muscle [8,9].

The presence of reactive groups in the central ethylenediamine residue has been also capitalized to produce positively charged poloxamines, independently of the pH [10] (Scheme 1B), mainly for improving the adhesion of cells when poloxamines are used

* Corresponding author at: The Group of Biomaterials and Nanotechnology for Improved Medicines (BIONIMED), Department of Pharmaceutical Technology, Faculty of Pharmacy and Biochemistry, University of Buenos Aires, 956 Junín St., 6th Floor, Buenos Aires CP1113, Argentina. Tel./fax: +54 11 4964 8273.
E-mail address: alesosnik@gmail.com (A. Sosnik).

0939-6411/$ - see front matter © 2010 Elsevier B.V. All rights reserved.
doi:10.1016/j.ejpb.2010.05.007

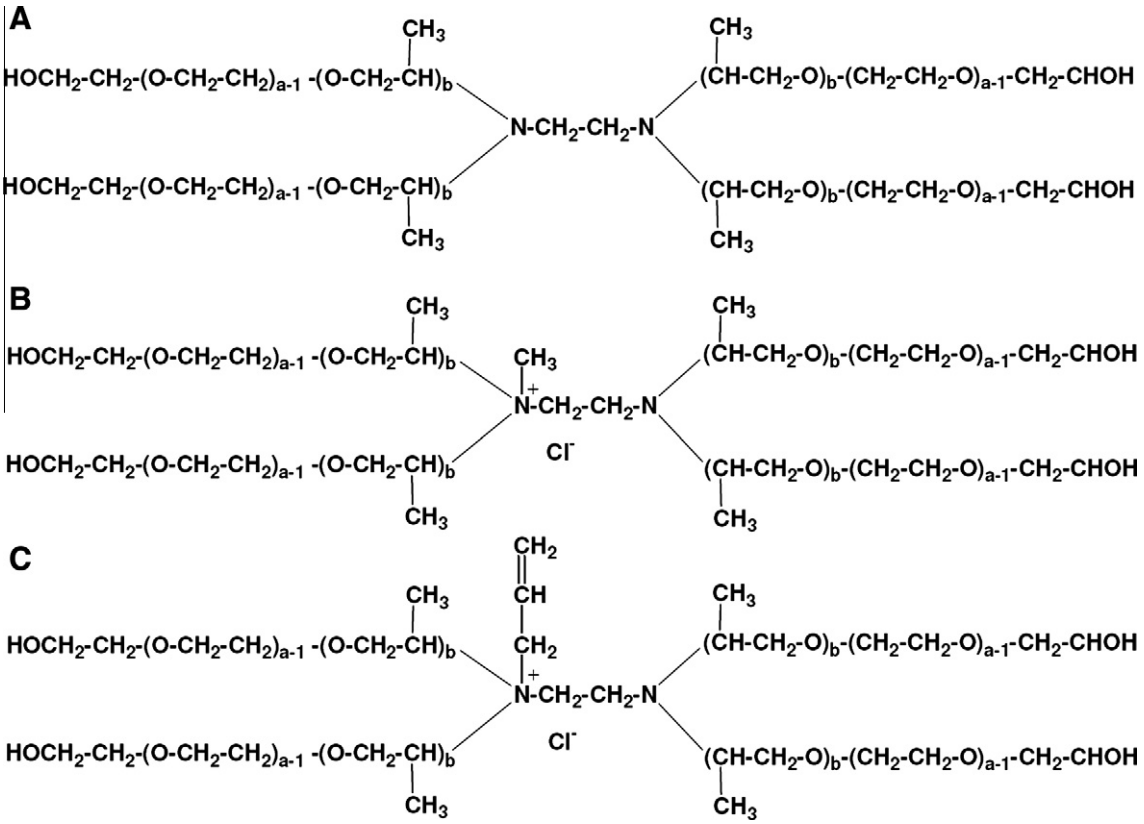

Scheme 1. Structures of (A) pristine poloxamine, (B) *N*-methylated poloxamine, and (C) *N*-allylated poloxamine.

as components of scaffolds for cell culture [10]. On the other hand, it was shown that *N*-methylation of Tetronic® 1107 (T1107) decreases the aggregation number and the micellar size with respect to the unmodified copolymer, probably due to a stronger repulsion of the central blocks of the copolymer and some steric hindrance caused by the bulky methyl group [4]. This *N*-methylated derivative showed higher solubilization and stabilization of the lactonic form of simvastatin as compared to the unmodified copolymer [4]. *N*-methylation of other poloxamines and *N*-alkylation with functional groups other than methyl is expected not only to further change the aggregation behavior of the copolymers in aqueous medium, but also to alter the physical stability under dilution and to modulate the drug/core interaction and the drug release profile.

In a recent work, we investigated the encapsulation process of the antiretroviral efavirenz (EFV) into polymeric micelles of pristine poloxamers and poloxamines and the pharmacokinetic behavior of the drug in rats, after oral administration (p.o.) [11]. EFV is a first-choice non-nucleoside reverse transcriptase inhibitor used in the High Activity Antiretroviral Therapy (HAART) of the infection by the Human Immunodeficiency Virus (HIV) [12] in both adults [13] and children [14]. Due to its high lipophilicity (log P = 5.4) and consequently poor aqueous solubility (4 μg/mL), the drug shows relatively low oral absorption and bioavailability (40–45%) and high inter-subject variability [15]. Furthermore, EFV is not commercially available worldwide in aqueous solution for the oral management of the pediatric pharmacotherapy. A commercial medium-chain triglyceride solution of EFV has shown lower oral bioavailability than the solid form. Preclinical studies indicated that the encapsulation of EFV in poloxamine micelles increases the C_{max} and the area-under-the-curve (AUC) [11] compared to the conventional triglyceride-based liquid formulation [16]. However, when the release profile was tested *in vitro* using the dialysis membrane method in intestine-like mimicking medium over 24 h, only 40% of the drug was released from the micellar reservoir. Conversely, approximately 60% of the drug loaded remained "sequestered" in the micelles probably due to the high physical stability of the drug-loaded micelles upon dilution and the strong drug/core interaction. Our hypothesis is that by making: (i) the micelles less stable under dilution (*N*-alkylation would strengthen the repulsion between positively-charged cores, thus accelerating the disassembly) and (ii) the efavirenz/micelle interaction weaker (due to the lower hydrophobicity of the core and the steric hindrance of the alkyl groups), the amount of drug released could be increased to a greater extent. This would result in higher oral bioavailability (Scheme 2).

The aim of this work was to elucidate the potential of *N*-alkylation of poloxamines as a strategy to modulate their self-assembly behavior in aqueous medium and the encapsulation and release of drugs. In this context, various *N*-methylated poloxamines, starting from poloxamines covering a wide range of EO/PO ratios and molecular weights, and an *N*-allylated poloxamine (from T1107; Scheme 1C) were synthesized and thoroughly characterized regarding their self-associative properties in aqueous media.

The cytocompatibility of the novel derivatives was studied and compared to that of the unmodified counterparts. Then, the encapsulation and *in vitro* delivery of EFV was evaluated. The incidence of drug loading on the micellar morphology and the physical stability of EFV-loaded micelles were studied in detail. The goal of *N*-allylation was to investigate whether the performance of the *N*-alkylated derivative exclusively relies on the positively-charged nature of the modified core or, by the contrary the molecular structure of the *N*-substituent (e.g., molecular volume) constitutes an additional parameter governing the process. These aspects, which are usually disregarded in most papers, are critical for the *in vivo* performance of a micellar-based formulation intended for oral administration [17].

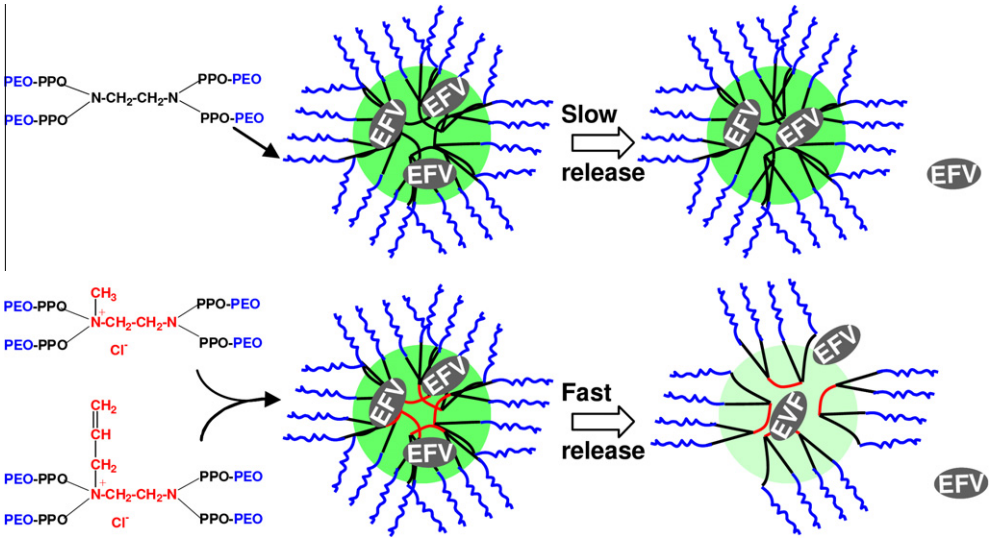

Scheme 2. Modulated efavirenz (EFV) release from *N*-alkylated poloxamines. (For interpretation of the references to color in this figure legend, the reader is referred to the web version of this article.)

2. Materials and methods

2.1. Materials

Poloxamines Tetronic® 901 (T901, batch USXW97149), 904 (T904, batch WSEZ78926), 908 (T908, batch WPYC566B), 1107 (T1107, batch WPOB646B), and 1307 (T1307, batch WPEA580B) were a gift of BASF Corporation (New Milford, CT) and used as received. Efavirenz (EFV) was from Laboratorio LKM SA (Buenos Aires, Argentina). Na_2HPO_4, citric acid, KCl, NaOH, K_2CrO_4, $AgNO_3$, H_2SO_4, HCl, $CDCl_3$ and solvents were of analytical grade. Purified water was obtained by reverse osmosis (MilliQ®, Millipore Iberica SA, Madrid, Spain). *N*-methylated derivatives of T901, T904, T908, T1107 and T1307 (met-T901, met-T904, met-T908, met-T1107 and met-T1307, respectively) were prepared as described elsewhere for met-T1107 [4,10]. A similar procedure was employed to synthesize *N*-allylated T1107 (allyl-T1107). Briefly, dry poloxamine T1107 (15.5 g, 0.001 mol) was dissolved in methanol (35 mL) and reacted with allyl iodide (Sigma–Aldrich, St. Louis, MO, USA, 3.44 g, 0.0205 mol, RT, 96 h) in darkness. The product was dried under vacuum in a rotary evaporator to remove methanol and allyl iodide residues. To exchange iodide by chloride, the crude was dissolved in water, and the solution was successively dialyzed against (i) distilled water (48 h), (ii) 2% NaCl (48 h), and (iii) ultra-pure water (72 h), using regenerated cellulose tubing (MWCO 1000 or 3500 depending on the molecular weight of the poloxamine; flat width 38 mm). Finally, the aqueous solution was freeze-dried (Labconco Co., Kansas City, MO). The degrees of *N*-methylation and *N*-allylation were determined by titration of chloride counterions using the argentometric method as described elsewhere [10]. Briefly, the pH was adjusted to 7–10 with H_2SO_4 or NaOH. Then, K_2CrO_4 indicator (1 mL, 5 wt.%) was added and the solution titrated with $AgNO_3$ solution (0.11 M) to a pink-yellow end point. The concentration of the $AgNO_3$ solution was previously determined with NaCl standard solution (0.015 N). Titrations were carried out in triplicate. Degrees of *N*-methylation and *N*-allylation were 44–45% and 67%, respectively.

Proton nuclear magnetic resonance (^{1}H NMR) analysis of *N*-allylated T1107 was performed in a Varian Mercury 300 MHz NMR spectrometer (Palo Alto, CA, USA; room temperature, DMSO-d_6 solution). To determine the % of *N*-allylation by this technique, the peaks at 6.05 ppm (allyl-group, CH_2=***CH***–CH_2–) and 1.00 ppm (PPO, –CH_2–CH(***CH_3***)–O, 233 protons) were considered. Determination of *N*-methylation extents by ^{1}H NMR was not possible because of the overlapping of the *N*-methyl group peak with that of PEO and PPO repeating units between 3 and 4 ppm.

Number- and weight-average molecular weights (M_n and M_w) and molecular weight distributions (M_w/M_n polydispersity, PDI) were determined by gel permeation chromatography (GPC) using a Waters GPC instrument (Milford, MA, USA) fitted with Ultrastyragel columns (conditioned at 25 °C) and a refractive index detector. Tetrahydrofuran (THF) was used as mobile phase at 0.9 mL/min. Polystyrene standards ranging from 2800 to 700,000 Da (Tokyo Soda Ltd., Tokyo, Japan) were used for calibration.

2.2. Preparation of copolymer solutions

The appropriate amount of copolymer was added to a given volume of in pH 5.0 buffer phosphate–citrate (0.0514 M Na_2HPO_4 and 0.0243 M citric acid) at 4 °C. Solutions were equilibrated at 20 °C for 24 h before the assays. Concentrations are expressed in % w/v.

2.3. Surface tension

The CMC of *N*-alkylated poloxamines was estimated from surface tension measurements. The analyses were carried out using the platinum ring method and a Lauda Tensiometer TD1 (Lauda-Königshofen, Germany), in triplicate, at 20 °C. CMC values of pristine poloxamines were determined for comparison.

2.4. Laser light scattering

Dynamic and static light scattering (DLS and SLS, respectively) intensities of aqueous solutions of modified poloxamines were measured at 20 and 37 °C using a laser light scattering instrument with vertically polarized incident light (λ = 488 nm, 2 W argon ion laser, Coherent Inc., Santa Clara, CA, USA) combined with a digital correlator (ALV 5000E, ALV GmbH, Langen, Germany). The intensity scale was calibrated against scattering from toluene. All solutions were filtered (0.2 μm, cellulose nitrate membranes, Whatman® GmbH, Dassel, Germany), directly placed into the cleaned scattering cell and equilibrated at 20 or 37 °C for 30 min. Measurements were made at a scattering angle θ = 90° to the incident beam for 5–15 min. Each experiment was repeated at least

twice. DLS correlation functions were analyzed using the CONTIN method to obtain the intensity distributions of decay rates [18]. Decay rate distributions gave distributions of apparent diffusion coefficient ($D_{app} = \Gamma/q^2$, $q = (4\pi n_s/\lambda)\sin(\theta/2)$, n_s = refractive index of solvent) and integrating over the intensity distribution gave the intensity-weighted average of D_{app}. The apparent hydrodynamic radius was calculated using the Stokes–Einstein equation:

$$r_{h,app} = kT/(6\pi\eta D_{app})$$

where k is the Boltzmann constant and η is the viscosity of water at temperature T.

The basis for analysis of SLS data was the Debye equation:

$$K^*c/(I - I_s) = 1/M_w + 2A_2c + \ldots\ldots$$

where I is the intensity of light scattering from the solution relative to that from toluene; I_s is the corresponding quantity for the solvent; c is the concentration (in g dm^{-3}); M_w is the mass-average molar mass of the solute; A_2 is the second virial coefficient (higher coefficients being neglected); and K^* is the appropriate optical constant for the instrument, which includes the specific refractive index increment of the solute, dn/dc, through the expression: $K^* = (4\pi^2/N_A\lambda^4)(n_B^2/R_B)(\mathrm{d}n/\mathrm{d}c)^2$, N_A being the Avogadro's number, n_B the refractive index of toluene (equal to $1.4969[1 - 5.7 \times 10^{-4}(T - 293)]$) [19], R_B the Rayleigh ratio of toluene (equal to $2.57 \times 10^{-5} \times [1 + 3.68 \times 10^{-3}(T - 298)]$ cm^{-1} with T in K) [20], and dn/dc the specific refractive index increment. Values of dn/dc and its temperature dependence were checked with an Abbé precision refractometer. The refractive indices of PEO and PPO are very similar, and within the error of determination (±0.004 cm^3/g), the values for the poloxamines were close to those reported for Pluronic block copolymers [21]. In addition, there was no consistent variation of dn/dc across the composition range of the copolymers. Therefore, an average value of 0.137 and 0.134 cm^3/g was used at 20 and 37 °C, respectively.

The mass-average association numbers of the micelles were calculated from:

$$N_w = \frac{M_w(micelle)}{M_w(molecule)}$$

where M_w (*molecule*) is the mass molecular weight of a single copolymer molecule as reported by BASF (Table 1) and M_w (*micelle*) is calculated from the intercepts of the Debye plots.

2.5. Cytocompatibility

2.5.1. Cells

BALB/3T3 clone A31 mouse embryonic fibroblast cells (CCL 163, ATCC) were maintained in GIBCO™ Dulbecco's Modified Eagle's medium (DMEM; Invitrogen Corp, Carlsab, CA) supplemented with 10% fetal bovine serum and gentamicin (52 μg/mL) at 37 °C in 5% CO_2 humidified atmosphere.

2.5.2. MTT cell growth assay

Cells were trypsinated and cultured in 96-well plates (2×10^4 cells/well). Autoclaved copolymer solutions in buffer phosphate pH 7.4 (final copolymer concentration 0.01%, 0.1%, 1% or 5%) were added and the cells incubated for 24 h [22]. The medium was soaked and replaced by fresh medium (200 μL) containing MTT (3-(4,5-dimethylthiazol-2-yl)-2,5-diphenyl-tetrazolium bromide) solution (20 μL, 5 mg/mL) and the well plates incubated for 4 h (37 °C, 5% CO_2) as stated in the cell growth determination kit MTT based (Sigma–Aldrich) used for the analysis. Immediately after incubation, the supernatant was removed, formazan crystals were dissolved (0.1 N HCl in anhydrous isopropanolol) and the absorbance measured within 1 h using a plate reader (Bio-Rad Model 680 Microplate Reader, Bio-Rad Laboratories (UK) Ltd., Herts, UK) at 570 nm. A sample of cells exposed to polymer-free culture medium was used as control (100% viability). Viability was calculated according to

$$\%\ \text{Viability} = (\text{Abs}_{sample}/\text{Abs}_{control}) \times 100$$

where Abs_{sample} and $\text{Abs}_{control}$ represent the absorbance of the sample of cell culture in the presence and in the absence of copolymer, respectively. The assays were carried out in triplicate.

2.5.3. LDH assay

Cell survival was also determined by means of the release of Lactate Dehydrogenase (LDH) using the cytotoxity detection Kit^{PLUS} (Roche, San Cugat del Vallès, Spain). Cells were cultured as previously depicted and the assay was carried out following the instructions of the kit. Triton X-100 (0.1%) and polymer-free culture medium were the positive control (total cell death) and the blank, respectively. Absorbance was measured in a plate reader at 490 nm and % viability calculated according to the instructions.

2.5.4. Live/dead assay

Cells cultured in a 24-well plate (2×10^5 cells/well) were exposed to T1307 and met-T1307 solutions (0.1% final copolymer concentration, 125 μL). After 24 h of incubation, cells were trypsinated and re-suspended in fresh DMEM. Cell suspensions were centrifuged in a cytocentrifuge (Zytokammer, Hettich Zentrifugen, Tuttlingen, Germany; 4×1 mL) to fix them to a microscope slide. Finally, cells were stained with a calcein AM/propidium iodide solution (Live/Dead Cell Viability Assay, Invitrogen) and visualized under a fluorescent microscope (Optiphot2, Nikon, Japan) with green and red filters. Image analysis software (Soft Imaging System, Version 3.2 Build 607) was used to estimate the viability based on the count of 200 cells.

Table 1
Structural properties and β values of different modified poloxamines. The degree of *N*-methylation and *N*-allylation was 44–45% and 67%, respectively. GPC data of pristine poloxamines is included for comparison.

Modified poloxamines	Molecular weight (kDa)[a]	M_n pristine poloxamine (kDa)[b]	PDI pristine poloxamine[b]	M_n *N*-alkylated poloxamine (kDa)[b]	PDI *N*-alkylated poloxamine[b]	N_{EO}[c]	N_{PO}[c]	Hydrophobic block (wt.%)	EO/PO molar ratio	β
Met-T901	4.7	8.5	1.01	8.5	1.01	2.7	18.2	90	0.15	6.68
Met-T904	6.7	9.6	1.01	9.0	1.04	15	17	60	0.88	2.29
Met-T908	25.0	9.6	1.12	10.5	1.05	114	21	20	5.4	0.77
Met-T1107	15.0	11.6	1.04	11.3	1.03	60	20	30	3.0	1.10
Allyl-T1107	15.0	11.6	1.04	11.3	1.03	60	20	30	3.0	1.10
Met-T1307	18.0	11.7	1.04	11.6	1.04	72	23	30	3.1	1.07

N_{EO}: mean number of EO units per PEO block; N_{PO}: mean number of PO units per PPO block; EO/PO: molar ratio of EO and PO units calculated as N_{EO}/N_{PO}.
[a] Average molecular weight of the pristine poloxamine as reported by BASF.
[b] Determined by GPC using polystyrene standards.
[c] From Ref. [4].

2.6. Encapsulation of EFV

EFV encapsulation assays were conducted at pH 5.0 and 20 °C to avoid EFV hydrolysis [11]. EVF (300 mg) was added to 10% micellar systems (6 mL) in glass vials (20 mL), and the samples were kept under magnetic stirring (700 rpm, Variomag; H + P Labortechnik AG, Oberschleissheim, Germany) at 20 °C for 72 h. Then, suspensions were filtered (0.45 μm cellulose nitrate membranes, Sartorius Stedim Biotech GmbH, Goettingen, Germany) to remove insoluble EFV. The concentration of the dissolved drug was determined by UV spectrophotometry (247 nm, Agilent 8453, Agilent Technologies Deutschland GmbH, Böblingen, Germany) by diluting 10 μL EFV-loaded micelle solution in 10 mL methanol, using a calibration curve of EFV (4–20 μg/mL range) methanolic solutions (correlation factor was 0.9998–1.0000). A drug-free copolymer solution in methanol was used as blank. The solubility factor (f_s) was calculated according to the equation:

$$f_s = S_a / S_{water}$$

S_a and S_{water} being the apparent solubility of EFV in each micellar system and the intrinsic solubility of the drug in a polymer-free pH 5.0 buffer (4 μg/mL), respectively. The solubilization capacity per gram of hydrophobic block was calculated using the mass fraction (wt.%) of the hydrophobic blocks in each copolymer. DLS studies were carried out as described for drug-free copolymer solutions.

2.7. Transmission electron microscopy (TEM)

Drug-free and drug-loaded 10% micellar systems (5 μL) were placed onto a copper grid covered with Fomvar film and, after 30 s, the excess was carefully removed. Then, phosphotungstic acid (5 μL, 2% w/v) was added and the excess removed after other 30 s. Finally, the sample was washed with water (5 μL, 30 s), dried in a closed container with silicagel and observed using a Philips CM-12 TEM apparatus (FEI Company, Eindhoven, The Netherlands).

2.8. Physical stability of drug-loaded micelles upon dilution

To estimate the physical stability of EFV-loaded micelles in gastric fluid, samples were diluted (1/75) in stomach-mimicking medium (HCl 0.1 N, measured pH 1.5) [23], incubated at 37 °C and the drug concentration monitored over time; 500 μL solution were diluted in 10 mL methanol and the concentration measured by UV as described in 2.6. The experiments were performed in triplicate.

2.9. In vitro release studies

EFV-containing micellar systems (10% copolymer) were diluted (1/10) in pH 5.0 buffer phosphate–citrate (0.0514 M Na_2HPO_4 and 0.0243 M citric acid) and aliquots (10 mL) placed into dialysis tubes (regenerated cellulose tubing, MWCO 3500), which were immersed into 900 mL of buffer phosphate saline (PBS, pH 7.4) at 37 °C. The external medium was replaced every 6 h in order to maintain sink conditions. The drug concentration in the internal solution (i.e., inside the dialysis bag) was monitored over time by UV spectrophotometry removing a small volume (100 μL) that was diluted in methanol (10 mL) in order to fit the calibration curve range (see Section 2.6). Assays were carried out in triplicate.

3. Results and discussion

3.1. Self-aggregation of N-alkylated poloxamines

Poloxamines display interesting structural features that enable the chemical modification of the micellar core by means of *N*-alkylation. In this framework, the first goal of the present work was to investigate extensively the impact of slight chemical modifications such as *N*-methylation and *N*-allylation on the self-aggregation behavior of these amphiphiles. On one hand, both alkylating agents lead to the formation of quaternary ammonium derivatives. On the other, the size of the new substituent may also influence their behavior. This parameter was evaluated by comparing methyl versus allyl moieties in T1107 derivatives. Five *N*-methylated derivatives were synthesized using iodomethane. Methylation extents were 44–45% (approximately one tertiary amine group out of two), as determined by argentometry. The *N*-allylation of T1107, which is described for the first time in the present paper, was carried out using allyl iodide. By argentometry, a higher alkylation extent (67%) was found, this finding being probably related to a less

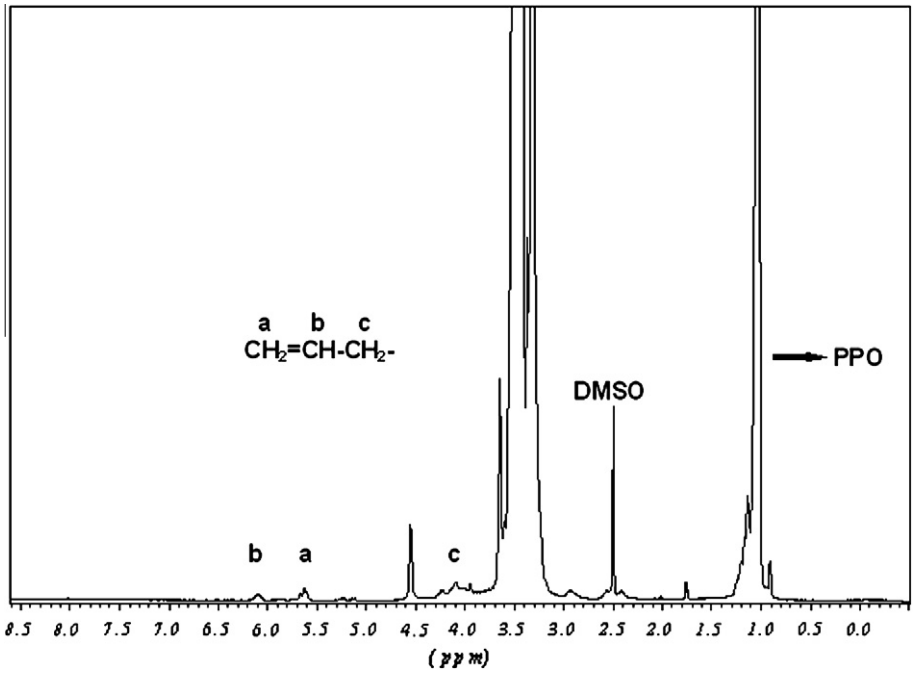

Fig. 1. ^{1}H NMR spectrum of allyl-T1107 in DMSO-d_6 showing the incorporation of the allyl moiety. The peak of DMSO at 2.50 ppm was used as reference.

bulky structure of the allyl moiety due to the presence of an unsaturated group. ^{1}H NMR analysis in DMSO-d_6 showed the presence of characteristic peaks of the vinyl group at 4.05 (CH_2═CH–***CH_2***–), 5.60 (***CH_2***═CH–CH_2–) and 6.05 (CH_2═***CH***–CH_2–) ppm (Fig. 1) [24]. The modification extent as determined by this method was 40%; the discrepancy between both techniques might be due to the inaccurate integration of the small peaks of allyl in the ^{1}H NMR spectrum.

Since the purification process by dialysis may alter the molecular weight and the molecular weight distribution, the different derivatives were analyzed by GPC and the number- and weight-molecular weight and the polydispersity determined (Table 1). It was previously reported that different batches of commercial copolymers may remarkably differ each other in mean molecular weight and polydispersity [25,26]. No relevant differences were found between pristine and dialyzed copolymers, although some discrepancies were observed when compared to the data reported by the supplier (Table 1). These deviations could stem from the use of different standards (polystyrene in our case, non-disclosed by the supplier). In absolute terms, the data provided by the manufacturer for the batches used in the present work should be more reliable. Our analysis just confirmed that, overall, the *N*-alkylation does not modify the molecular weight of the copolymer.

The hydrophobicity of the copolymers was estimated using the parameter β, i.e., the ratio between the Flory radius of the PPO and the PEO blocks [27].

$$\beta = \frac{I_{PO}(N_{PO})^{3/5}}{I_{EO}(N_{EO})^{3/5}}$$

In this equation, N_{PO} and N_{EO} represent the numbers of PO and EO units, respectively, and I_{PO} and I_{EO} are the atomic distances between C1 and C3 plus C3 and O of the PO (5.1 Å) and between C1 and O of the EO (2.4 Å) units [27]. The potential effect of the protonation or the *N*-alkylation on the hydrophilicity of the unimers is not taken into account in β calculation. Based on the β values for the pristine materials, the modified poloxamines were classified into three groups: (i) highly hydrophilic ($\beta \approx 1$, met-T908, allyl-T1107, met-T1107, and met-T1307), (ii) of intermediate polarity ($\beta \approx 2$, met-T904) and (iii) highly hydrophobic ($\beta > 6$, met-T901) (Table 1). The extent of micellization of the different derivatives was determined from surface tension measurements.

The copolymers can be divided into two groups according to the plots of surface tension versus copolymer concentration (Fig. 2). The surface tension patterns of the hydrophilic copolymers displaying the lowest β values, namely met-T908, allyl-T1107 and met-T1307, were quite similar to each other and were in good agreement with the behavior of met-T1107 reported elsewhere [4]; surface tension decreased sharply to concentration values around 0.1 mM. Above this concentration no additional change in surface tension was observed. For a similar copolymer concentration, the higher the N_{PO} value, the lower the minimum surface tension; i.e., the values for 0.1% met-T908 (N_{PO} = 21) and met-T1307 (N_{PO} = 23) systems were 47.4 and 43.3 mN/m, respectively (Fig. 2). The profile of allyl-T1107 (N_{PO} = 20) was almost superimposable to that of met-T908. This behavior was in agreement with that shown by unmodified poloxamines [3,4]. In contrast, copolymers of intermediate to high β value (met-T901 and met-T904) displayed a gradual decrease of the surface tension as the copolymer concentration increased; met-T901 being the most surface active.

The CMC was established as the copolymer concentration above which the surface tension showed a less pronounced change, indicating the formation of micelles (Table 2). This criterion is usually followed in the case of copolymers that display surface tension plots with several regions of changing slopes, deviating from the common model [28]. Different slopes in the semilogarithmic plot (Fig. 2) might reflect conformational changes to enable more copolymer molecules to reach the interface, as previously reported for some poloxamers [29]. The CMC values of pristine poloxamines reported in Table 2 are in close agreement with those previously estimated from pyrene fluorescence measurements [4].

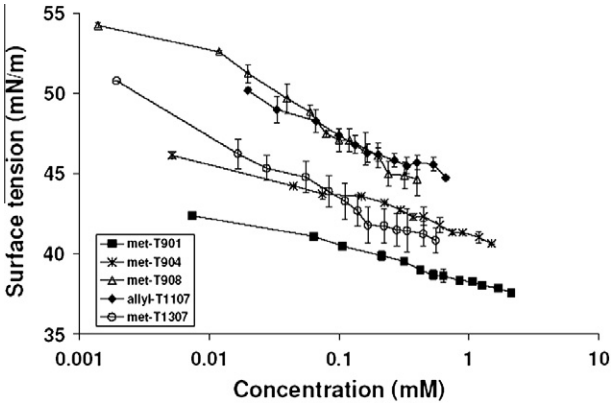

Fig. 2. Surface tension plots of *N*-alkylated poloxamines in buffer phosphate–citrate (pH 5), at 20 °C. The surface tension of the buffer without copolymer was 73.5 mN m.

Independently of the β value, the lowest the molecular weight of the copolymer, the highest the concentration required for micellization; e.g., CMC of met-T901, met-T904 and met-T1307 was 0.84, 0.74 and 0.17 mM, respectively. In other words, the number of molecules required to diminish the surface tension is higher for copolymers of lower molecular weight. This phenomenon was also apparent for copolymers showing similar EO/PO ratios. On the other hand, the higher CMC value of met-T908 with respect to met-T1307 indicates that the influence of the hydrophilic–lipophilic balance cannot be neglected; T908 contains 80 wt.% PEO. It is worth mentioning that CMC values of the modified poloxamines were of the same order of magnitude as those shown by unmodified counterparts. However, *N*-alkylation led to a moderate decrease of the aggregation tendency as supported by the higher CMC values observed (Table 2). This phenomenon is consistent with a stronger repulsion between quaternized unimers [4]. The effect of the number of EO units (ranging from 3 to 114 EO units) on CMC was also small (Table 2), in full agreement with the behavior of the pristine poloxamines [4]. Finally, despite positively charged poloxamines may find self-assembly difficult [2], *N*-alkylated poloxamines do generate micelles at relatively low concentrations, comparable to those of the pristine copolymers.

Table 2
CMC values of pristine and *N*-alkylated poloxamines estimated from surface tension measurements in buffer phosphate–citrate (pH 5), at 20 °C.

Poloxamine	CMC (% w/v)	CMC (mM)
T901	0.30	0.64
T904	0.50	0.75
T908	0.40	0.16
T1107	0.20	0.13
T1307	0.20	0.11
Met-T901	0.40	0.84
Met-T904	0.50	0.74
Met-T908	0.60	0.24
Met-T1107	1.01[a]	0.67 [a]
Allyl-T1107	0.50	0.33
Met-T1307	0.30	0.17

[a] Data taken form Ref. [4].

3.2. Micellar size and aggregation number

The hydrodynamic radius and size distribution of the micelles were obtained by DLS using a copolymer concentration (10%) well above the CMC in order to ensure that most polymer chains are forming polymeric micelles and that the number of micelles is enough for an accurate determination of their mean average size. Intensity fraction distributions of log $r_{h,app}$ for *N*-alkylated poloxamines at 20 °C displayed several peaks: the first peak (e.g., peak 1 in Fig. 3A) corresponds to copolymer unimers, since at this temperature the micellar equilibrium is shifted to unimers, as confirmed by the tiny peak corresponding to copolymer micelles (peak 2). A third intense peak (peak 3) at longer radii could be ascribed to insoluble polymeric material resulting from copolymer synthesis, as reported for Pluronic [30]. Since intensity-weighted distributions are being plotted and the intensity is proportional to the square of the molecular weight, the large insoluble polymeric clusters, even at small proportions, contribute importantly to the scattered intensity. At 37 °C, the peak corresponding to the micelles is enhanced at the expense of that of unimers and insoluble clusters. This observation points out that the micelles become the predominant species as temperature rises due to the dehydration of both PPO and PEO blocks. Furthermore, as micelles are more numerous, they can partially incorporate the insoluble polymeric material forming large clusters at lower temperature. Thus, the polydispersity index decreases from 0.30 to 0.15 when temperature increases from 20 to 37 °C. The small width of the peak assigned to micelles (Fig. 3B) indicates that the unimers closely associate with micelles, as reported for other copolymers [31,32].

The analysis of SLS data using the Debye equation with light scattered at 90° requires that the micelles are small relative to the wavelength of the light. The maximum apparent hydrodynamic radius measured was of approximately 8 nm; hence, a correction factor to M_w of not more than 1.02% is required [33,34]. In fact, measured values of the angular dissymmetry factor, I_{45}/I_{135}, for the micellar copolymer solutions were 1.04 or less, which is consistent with a small intra-particle scattering factor. Therefore, a correction on this regard was not needed.

The Debye equation truncated to the second term, A_2, was not used to directly analyze the SLS data, because micellar interaction resulted in inter-particle interference leading to significant curvature of the Debye plot even in the low concentration range. This feature is illustrated in Fig. 4, which shows data for two copolymers in solution at 37 °C. Thus, the curves were fitted using a procedure based on the scattering theory for hard spheres [35–37] whereby the inter-particle interference factor (structure factor, *S*) in the scattering equation

$$K^*c/(I - I_s) = 1/SM_w$$

was estimated as

$$1/S = [(1 + 2\phi)^2 - \phi^2(4\phi - \phi^2)](1 - \phi)^{-4}$$

ϕ being the volume fraction of equivalent uniform spheres. Values of ϕ were calculated from the volume fraction of copolymer in the system by applying a thermodynamic expansion factor $\delta_t = v_t/v_a$, where v_t is the thermodynamic volume of a micelle (*i.e.*, one eighth of the volume, v, excluded by one micelle to another) and v_a is the anhydrous volume of a micelle ($v_a = vM_w/N_A$, v being the partial specific volume of the unimer). The fitting parameter, δ_t, applies as an effective parameter for compact micelles irrespective of their exact structure. This method is equivalent to the use of the virial expansion for the structure factor of effective hard spheres taken to its seventh term, but just requires two adjustable parameters, *i.e.*, M_w and δ_t [35–37]. The micellar parameters of *N*-alkylated poloxamines coming from fitting the experimental data to theory for hard spheres are listed in Table 3 (the goodness of the fitting is shown in Fig. 4 for two poloxamine derivatives). At 20 °C, highly hydrophilic met-T908, met-T1107 and allyl-T1107 were mainly in the form of unimers ($N_W = 1$) and the thermodynamic parameters were not calculable. More hydrophobic or larger copolymers (e.g., met-T904 and met-T1307) showed a slightly higher self-aggregation tendency and formed dimers ($N_W = 2$). Small hydrodynamic radii were also consistent with the presence of unimolecular and dimolecular aggregates. It is worth remarking that copolymer concentrations were above the CMC calculated from surface tension measurements. However, data indicated that under these conditions the unimer:micelle equilibrium is clearly shifted toward the unimeric form. *N*-alkylation increased the electrostatic repulsion among poloxamine molecules and clearly made the self-aggregation difficult, resulting in lower aggregation numbers at

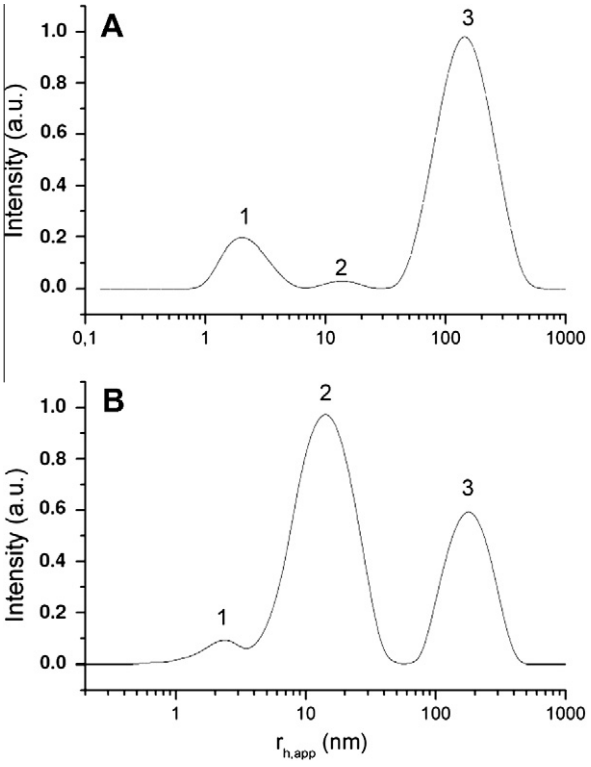

Fig. 3. Intensity fraction size distributions of the apparent hydrodynamic radius of 10% met-T1307 at (A) 20 °C and (B) 37 °C, as measured by DLS.

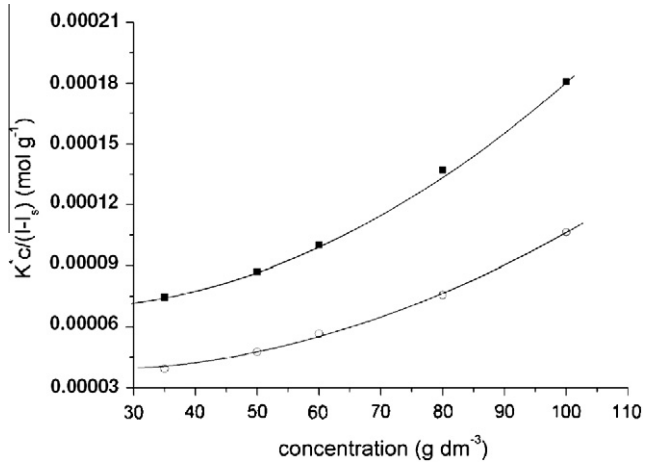

Fig. 4. Debye plots for micellar solutions of copolymer met-T1107 (solid symbols) and copolymer met-T904 (open symbols) at 37 °C.

Table 3
Micellar parameters of *N*-alkylated poloxamines in buffer phosphate–citrate (pH 5) at 20 and 37 °C.

Poloxamine	T (°C)	N_w	r_h (nm)	δt	r_t (nm)	r_c (nm)	v_e (nm^3)	n_w
Met-T901	20	15	6.7	1.8	3.6	2.9	7	232
Met-T904		2	2.2	1.2	1.8	1.4	0.3	7
Met-T908		1	2	–	–	–	–	–
Met-T1107		1	2.6	–	–	–	–	–
Allyl-T1107		1	2.2	–	–	–	–	–
Met-T1307		2	3.2	1.3	2.6	1.6	0.2	3
Met-T901	37	–	–	–	–	–	–	–
Met-T904		10	5.1	1.9	3.5	2.4	0.87	27
Met-T908		2	3.4	1.6	3.1	1.5	0.17	4
Met-T1107		4	5.4	2.2	3.6	1.9	0.73	22
Allyl-T1107		3	5.4	2.5	3.4	1.7	0.49	14
Met-T1307		6	8.1	2.5	4.5	2.2	1.30	43

N_w: micellar aggregation number, r_h: hydrodynamic radius, δt: expansion factor, r_t: thermodynamic radius, r_c: radius of micellar core, v_e: volume of the hydrated EO unit, n_w: number of water molecules associated with each EO unit.

pH 5.0 than those found for pristine poloxamines at pH 2.0 [4]. This clearly proves the interference of the permanent positive charge on the micellization process.

The highly hydrophobic pristine T901 precipitates in water and forms cloudy systems that hampered the measurement of the different micellar parameters by SLS [4]. In contrast, at 20 °C, met-T901 showed slightly higher solubility than the un-methylated derivative, and the formation of micelles of N_w 15 and r_h 6.7 nm was established.

The copolymers showed a higher tendency to self-aggregate at 37 °C. The hydrophobic met-T901 formed large and insoluble clusters that could not be measured, while intermediate to highly hydrophilic *N*-alkylated copolymers rendered polymeric micelles. *N*-alkylation with different moieties resulted in a differential behavior; i.e., N_w values of met- and allyl-T1107 were 4 and 3, respectively. This behavior may stem from the different molecular volume of the *N*-substituents and *N*-alkylation extents. These findings were also in agreement with a previous work that showed lower N_w of met-T1107 when compared to the pristine molecule [4]. Due to a lower protonation extent and a consequently stronger self-assembly driving force [38], a pH increase led to a higher *N* also for *N*-alkylated poloxamines; i.e., N_w values were 3 and 4 for met-T1107 at pH-values of 4.0 and 5.0, respectively.

On the other hand, assuming the mean length of a PO and EO unit to be *ca.* 0.36 nm and neglecting the size of the diamine unit, the average core volume (v_c) and core radius (r_c) of a copolymer micelle can be estimated as

$$v_c = (4/3)\pi \cdot r_c^3 = n \cdot v_{PO} \cdot N_w$$

where n is the length of the hydrophobic block and v_{PO} is the volume of a PO unit

$$v_{PO} = M_{w,PO}/\rho_{PO} \cdot N_A$$

$M_{w,PO}$ and ρ_{PO} being the molar mass and the density of a PO unit, respectively, assuming spherical micelle cores with no penetration of water.

Accordingly, with the assumption that micelles have a spherical shape with a liquid-like core free of solvent [39], further evaluation of the extent of drainage of the micellar corona could be performed. The volume of each solvent swollen EO unit, v_E, could be estimated from the relation

$$(4/3)\pi(r_t^3 - r_c^3) = mN_w v_E = \langle L_h \rangle$$

where L_h is the micellar corona thickness and v_E the volume of each solvent swollen EO unit. Considering that the volume of a non-swollen liquid EO unit is 0.073 nm^3 and that the volume of a water molecule is close to 0.030 nm^3, the number of water molecules associated with each EO unit, n_w, was also estimated (Table 3).

Morphological characterization of *N*-alkylated poloxamine micelles was complemented with TEM analysis (Fig. 5). Micelles showed the characteristic spherical morphology and the co-existence of aggregates of different sizes. It is noteworthy that water evaporation during sample preparation and shrinkage of the structures usually leads to size underestimation. Conversely, the inclusion of hydration water molecules in the calculation of the average size by DLS overestimates the dimensions of the aggregates. Taking these facts into consideration, light scattering and TEM data were in good agreement.

3.3. Cytocompatibility of pristine and N-alkylated poloxamines

Although the cytocompatibility of some pristine poloxamines and of met-T1107 has been previously evaluated in the context of tissue engineering applications [10,40–43], the paucity of information about most poloxamines and the several pathways that can be responsible for cytotoxic phenomena advise us to gain insight

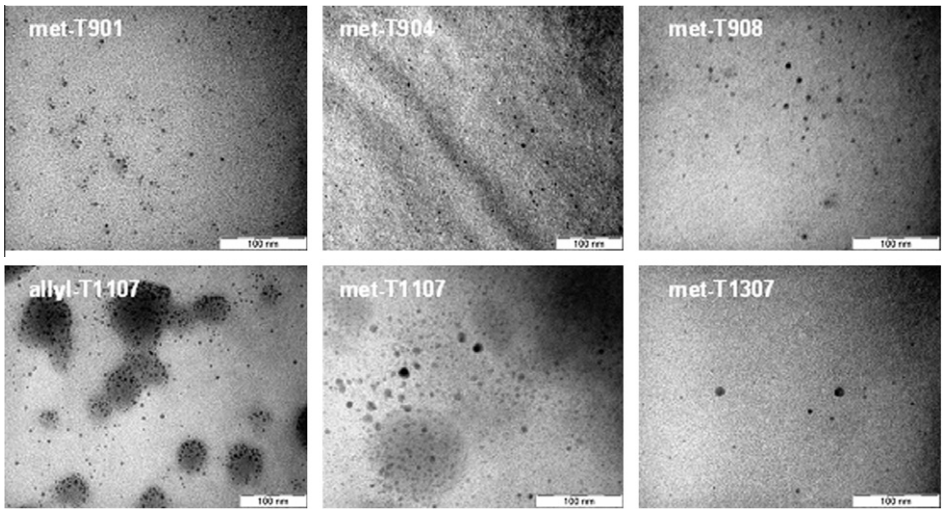

Fig. 5. TEM micrographs of 10% modified poloxamine solutions prepared in buffer phosphate–citrate (pH 5.0) and negatively stained with 2% phosphotungstic acid. Scale bar = 100 nm.

into this issue. The cellular response to the unmodified and *N*-alkylated poloxamines was evaluated on a murine fibroblast cell line by two different methods. The LDH assay enabled to measure if this cytosolic enzyme was released to the culture medium due to increased membrane permeability, indicating cell damage or lysis [44]. Low copolymer concentration systems showed viability extents close to 100%, the viability of T901 and met-T901 being slightly lower (Fig. 6A). Highly hydrophilic pristine and *N*-alkylated poloxamines showed high viability levels (>90%) in the whole range of concentrations. Copolymers of intermediate to high hydrophobicity (T901, met-T901, T904, and met-T904) showed a gradual viability loss as the copolymer concentration rose. This effect was especially noticeable for the *N*-methylated derivatives; e.g., viability in presence of 1% T901 and met-T901 was 55.6% and 27.2%, respectively. In general, the higher the β value, the more cytotoxic the effect found. This behavior could stem from the greater affinity of the amphiphile for cellular membrane structures, increasing cell permeability. Inhibition of *P*-glycoprotein activity by hydrophobic poloxamers is been thought to occur due to the intercalation of poloxamer in the cellular membrane and its fluidization [45]. Precipitation of cholesterol by highly hydrophobic poloxamines T701 and T702 has been also reported [46]. In contrast, hydrophilic copolymers would display lower affinity and, consequently, lower cytotoxicity [47]. To further investigate the cytocompatibility of these copolymers, the activity of the mitochondrial dehydrogenase enzyme was studied by means of the MTT assay [22]. Both T901 and met-T901 were highly cytotoxic, even at copolymer concentrations as low as 0.01%, the viability being <20% (Fig. 6B). In contrast, the other poloxamines and *N*-alkylated counterparts showed relative good viability, the levels ranging between 70% and 100% for concentration of 0.01%. The *N*-alkylated poloxamines exhibited a slight decrease in the cytocompatibility; e.g., 0.01% met-T1307 had 50% viability. It is worth remarking that 50% has been previously stated as a reference value to indicate cytotoxicity [48]. A gradual decrease in the viability was apparent for greater concentrations. For example, cells exposed to 0.1 and 1% met-T904 underwent a sharp viability loss to final levels of 22% and 16%, respectively. In contrast, T908 and T1107 showed viability extents around 60% even when the concentration was as high as 5%. These findings stressed the relevance of doing both

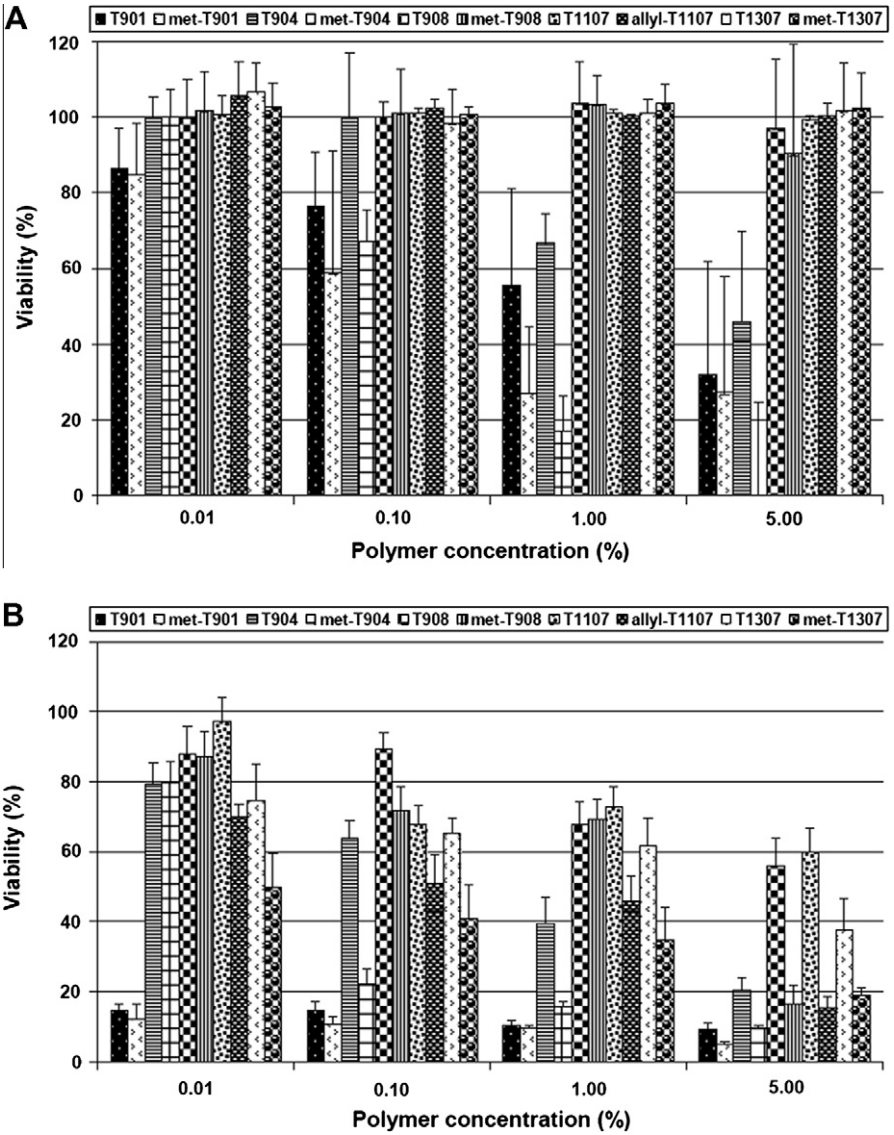

Fig. 6. Viability of BALB/3T3 fibroblasts exposed to different pristine and *N*-alkylated poloxamine solutions. LDH assay (A) and MTT (B) assay. Results are expressed as mean ± s.d. (n = 3).

cytotoxicity and cytoviability tests to elucidate the cytocompatibility of a given material. Finally, the live/dead assay of cells exposed to 0.1% T1307 and met-T1307 showed 92% and 96% viability, respectively, confirming the high cytocompatibility of *N*-alkylated derivatives of highly hydrophilic copolymers (Fig. 7). The cytotoxicity of poloxamines may be overestimated *in vitro*; cells are not protected by the anatomical barriers present *in vivo* [49]. However, these *in vitro* cytocompatibility studies, which constitute the most extensive ones conducted with poloxamines and their *N*-alkylated derivatives, enabled the generation of a biocompatibility ranking. Such a ranking may be useful for selection of copolymers combining good encapsulation capacity and an appropriate compatibility profile for use in the development of drug delivery systems in general and for oral administration in particular.

3.4. EFV encapsulation and effect on the self-aggregation

Pediatric HIV is highly prevalent infectious disease in the developing world [50]. Approximately 90% of the HIV-positive children do not afford an appropriate antiretroviral (ARV) pharmacotherapy. Moreover, only 2% of the 2 million patients in the sub-Saharan region (sSR) have access to medication; sSR is the most affected area. One of the main reasons for this dramatic situation stems from the fact that only 12 ARVs are approved for pediatric treatment as opposed to the 25 available for adults [51]. Furthermore, most of the drugs are not commercially available in liquid form [52]. Thus, the only alternative to treat neonates and infants is to develop extemporaneous (namely unlicensed) medicines [53,54]; this practice has risen serious quality, safety and efficacy concerns, especially in constrained-setting countries [55–57]. Accordingly, there exists an urgent need to develop innovative and cost-affective liquid formulations for HIV and other infectious diseases of developing nations that enable both dose adjustment to body weight and easy swallowing and display an optimized oral pharmacokinetic performance and patient compliance [58,59]. The World Health Assembly has called pharmaceutical companies and research groups in academia to develop formulations that fulfill the conditions for pediatric administration in HIV, tuberculosis (TB), HIV/TB co-infection, etc. [60]. EFV is among the first-line ARVs used in the pediatric cocktail and the only liquid formulation is a 30 mg/mL medium-chain triglyceride solution [61] that displays lower oral bioavailability and probably high inter-subject variability than the solid form. In this framework, our goal is to explore the clinical potential of a highly concentrated EFV aqueous solution [11].

Solubility assays were carried out at a copolymer concentration (10%) far above the CMC (Table 2). Due to the limited solubility of T901 and met-T901 *per se* and their apparently poor cytocompatibility, these copolymers were not included in this study. Pristine and *N*-alkylated derivatives substantially improved the solubility of EFV; T904 and met-T904 being the most efficient copolymers (Table 4). S_a values for the pristine and the quaternized copolymer were 29.70 and 28.68 mg/mL, respectively, representing 7425- and 7170-fold increases. These solubilization improvements are the highest ever reported for EFV by any nanocarrier in aqueous medium. Conversely, copolymers with the highest PEO content and the lowest β value (T908 and met-T908) showed the lowest ability to solubilize EFV, probably due to their lower micellization tendency and the extremely low concentration of micelles. Derivatives of slightly higher β showed a better solubilization performance, the f_s being 1385, 2035 and 3155 for met-T1107, allyl-T1107 and pristine T1307, respectively (Table 4). Due to the inverse thermoresponsive behavior of these copolymers, the solubilization extents found at 23 °C were greater than those reported at 20 °C for unmodified poloxamines [11]; i.e., f_s values increased 1.5- and 1.8-fold for T1307 and T1107, respectively. This relies on the fact that the higher the temperature, the higher the concentration of micelles. Interestingly, *N*-alkylation decreased the solubilization capability of all the derivatives, due to a lower micellization tendency and a reduced drug/core interaction. This phenomenon was particularly remarkable for amphiphiles displaying a lower β value. For example, S_a values were 1.61 (f_s = 402.4) and 0.67 mg/mL (f_s = 166.9) for T908 and met-T908, respectively. In the case of copolymers with similar β (T1107 and T1307), the higher the molecular weight, the lower the influence of the chemical modification on solubilization. Despite most of the copolymer molecules were in the form of unimers in solution without EFV (Table 3), the sharp increase in the solubility suggests that the presence of EFV promotes the self-aggregation of the amphiphile.

Table 4
EFV solubilization parameters for drug-saturated 10% poloxamine solutions in buffer phosphate–citrate (pH 5) at 20 °C.

Poloxamines	EFV in different poloxamines micellar systems (10%)		
	S_a (mg/mL) (±SD)	f_s (±SD)	mg EFV/g hydrophobic block (±SD)
T904	29.70 (1.04)	7425.9 (260.5)	495.1 (17.4)
Met-T904	28.68 (2.14)	7170.9 (534.7)	478.1 (35.7)
T908	1.61 (0.19)	402.4 (48.2)	80.5 (9.6)
Met-T908	0.67 (0.02)	166.9 (3.9)	33.4 (0.8)
T1107	11.04 (0.76)	2760.5 (189.9)	368.1 (25.3)
Met-T1107	5.54 (0.43)	1385.4 (107.5)	184.7 (14.3)
Allyl-T1107	8.14 (0.33)	2035.1 (81.6)	271.4 (10.9)
T1307	12.62 (0.20)	3155.3 (50.1)	420.7 (6.7)
Met-T1307	9.86 (0.40)	2466.1 (99.3)	328.8 (13.3)

S_a: EFV apparent solubility; f_s: EFV solubility factor.

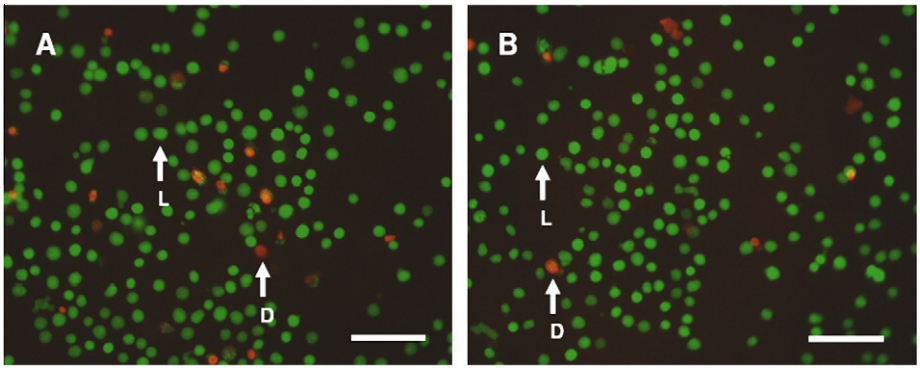

Fig. 7. Viability of BALB/3T3 fibroblast cells cultured for 24 h on T1307 0.1% (A), and met-T1037 0.1% (B). Live cells (L) stained with calcein AM appear in green and dead cells (D) stained with propidium iodide appear in red are pointed out with arrows. Scale bar = 100 μm. (For interpretation of the references to color in this figure legend, the reader is referred to the web version of this article.)

N-allylation had a lower detrimental effect than *N*-methylation, regardless the higher alkylation extent; S_a values for met- and allyl-T1107 were 5.54 and 8.14 mg/mL, respectively. These results also pointed out that the steric hindrance of the alkyl moiety is a key player that governs the process, this phenomenon being more prominent in the hydrophilic copolymers. In contrast, T904 and met-T904 showed very similar performances (only a slight decrease due to methylation). This result is especially remarkable, considering the low molecular weight and the high charge/mass ratio of met-T904. Interestingly, a linear dependence of S_a versus % of hydrophobic blocks in the copolymer was observed (S_a = 0.6856 × −11.631 (% hydrophobic blocks); R^2 = 0.9619) (Fig. 8). This would eventually enable the prediction of the solubilization capacity of EFV by other poloxamine derivatives.

3.5. Effect of EFV on the size of the aggregates

Micellar size and size distribution dictate the interaction of the nanocarriers with cells, modifying the biodistribution profile [62]. As stressed before, EFV-loaded micelles are intended for oral administration [11,63]. Drug incorporation into the micelles may result in an increase of the micellar size due to (i) the enlargement of the micellar core [64,65] and (ii) the fusion of drug-containing micelles into larger ones (secondary aggregation) [6,66]. Furthermore, changes in the aggregation pattern can be envisioned due to the presence of EFV. The size and size distribution of EFV-loaded 10% *N*-alkylated poloxamine micelles were measured by DLS (Table 5). Data of drug-free micelles at 20 °C indicated that regardless of the fact that the concentration is above the CMC, the copolymers are predominantly as unimers of hydrodynamic radii between 2 and 3.2 nm (Table 3). In contrast, although a small fraction of unimers still persists, drug-loaded systems evidenced the formation of regular and enlarged micelles; i.e., met-T904 and met-T1107 showed r_h of 11 and 24.3 nm, respectively. Remarkably, met-T908 formed micelles of pronouncedly larger size, 59 nm. Together with solubilization data (Table 4), these findings confirm that the presence of EFV induced the self-aggregation of the poloxamines. At 37 °C, results were consistent with the expansion of the micelles. For example, drug-loaded met-T1107 and allyl-T1107 micelles showed r_h values of 9.0 and 7.1 nm, respectively, as opposed to 5.4 nm sizes shown by drug-free systems. In addition, met-T908 showed three size populations that correspond to unimers (r_h = 2.7 nm) and enlarged micelles (r_h = 18.5 and r_h = 160 nm). Met-T1307 showed a similar aggregation pattern, though due to a higher β value unimers were almost absent. The remarkable difference in the aggregation pattern of drug-free and drug-loaded micelles at 37 °C is exemplified in Fig. 9.

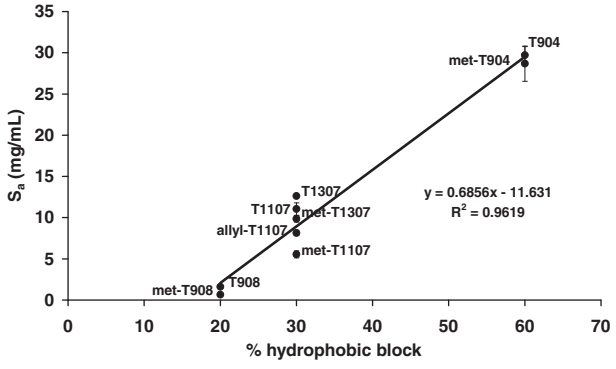

Fig. 8. Efavirenz apparent solubility (S_a) in 10% poloxamine solutions versus the content in hydrophobic units (wt.%) of poloxamines.

Table 5
Micellar size and size distribution of EFV-loaded 10% *N*-alkylated poloxamine solutions.

Poloxamine	*T* (°C)	Peak 1		Peak 2		Peak 3	
		r_h (nm)	%	r_h (nm)	%	r_h (nm)	%
Met-T904	20	–	–	11.0	100.0	–	–
Met-T908		2.0	16.6	7.0	0.2	59.0	83.2
Met-T1107		4.3	4.8	24.3	95.2	–	–
Allyl-T1107		2.4	9.1	23.6	90.9	–	–
Met-T1307		2.3	3.3	22.0	66.7	130.4	30.0
Met-T904	37	–	–	9.0	100.0	–	–
Met-T908		2.7	20.8	18.5	37.5	160.0	41.7
Met-T1107		–	–	9.0	100.0	–	–
Allyl-T1107		–	–	7.1	91.7	126.0	8.3
Met-T1307		2.1	5.5	11.5	61.0	161.0	33.5

3.6. Physical stability of drug-containing micelles upon dilution

Drug-loaded micelles undergo dilution in body fluids after administration, which may result in micellar disassembly and drug precipitation. The modulation of this phenomenon could be capitalized to increase the drug release rate and attain higher absorption after oral administration. Since EFV is an orally administered drug, evaluating the physical stability of the EFV-loaded micelles under dilution in gastric-like medium (HCl 0.1 N, 37 °C) was of interest. Previous investigations confirmed the chemical stability of EFV under the conditions of the study [11]. Systems displaying the highest solubilization capacity (T904, met-T904, T1107, allyl-T1107, T1307 and met-T1307) were diluted (1/75) and the drug concentration was monitored over time. In all the cases, final copolymer concentrations were below the CMC values and the poloxamines were in diprotonated form. Only the remaining non-quaternized tertiary amine groups of *N*-alkylated derivatives behave as pH-dependent. All the systems remained physically stable until day 3, the EFV solubility being above 90% of the initial value (Fig. 10). As opposed to T1307 that showed high stability over time, met-T1307 micelles gradually lost EFV, 80% remaining at day 7. T904 and met-T904 micellar systems also showed a slight EFV concentration loss, the *N*-methylated-based system being less physically stable than the pristine one. EFV-loaded T1107 and allyl-T1107 micellar systems were highly stable.

3.7. In vitro release studies

One of the goals of *N*-alkylation was to alter the drug/core interaction and, by doing this, to modulate the drug release from the micellar reservoir for maximizing the amount of released drug in the gastrointestinal tract. To characterize the release profile of the different systems and to compare them to those of the unmodified poloxamines, EFV-loaded 10% copolymer solutions were diluted (1/10 in buffer phosphate–citrate, pH 5) and dialyzed against buffer phosphate saline (pH 7.4) and the concentrations monitored over 24 h (Fig. 11). The MWCO of the dialysis tube ensured that no micellar diffusion occurred. Analysis of release data indicated that, after an initial burst at 0–2 h, the profile fits to a zero-order-kinetics (R^2 > 0.966, Table 6). The *N*-alkylated systems released EFV more rapidly than the pristine micelles (Fig. 11). For example, T904 released 15% after 12 h, while met-T904 released 19%. These findings were in agreement with the lower stability of EFV-loaded met-T904 micelles (Fig. 10). The incidence of *N*-alkylation on EFV release rate was even more remarkable for T1107 systems; *N*-methylated or *N*-allylated copolymer showed a sharp increase in the total released amount at 24 h (48% or 77%, respectively) compared to the pristine copolymer (36%). Thus, regardless the high stability at 37 °C of EFV-containing allyl-T1107

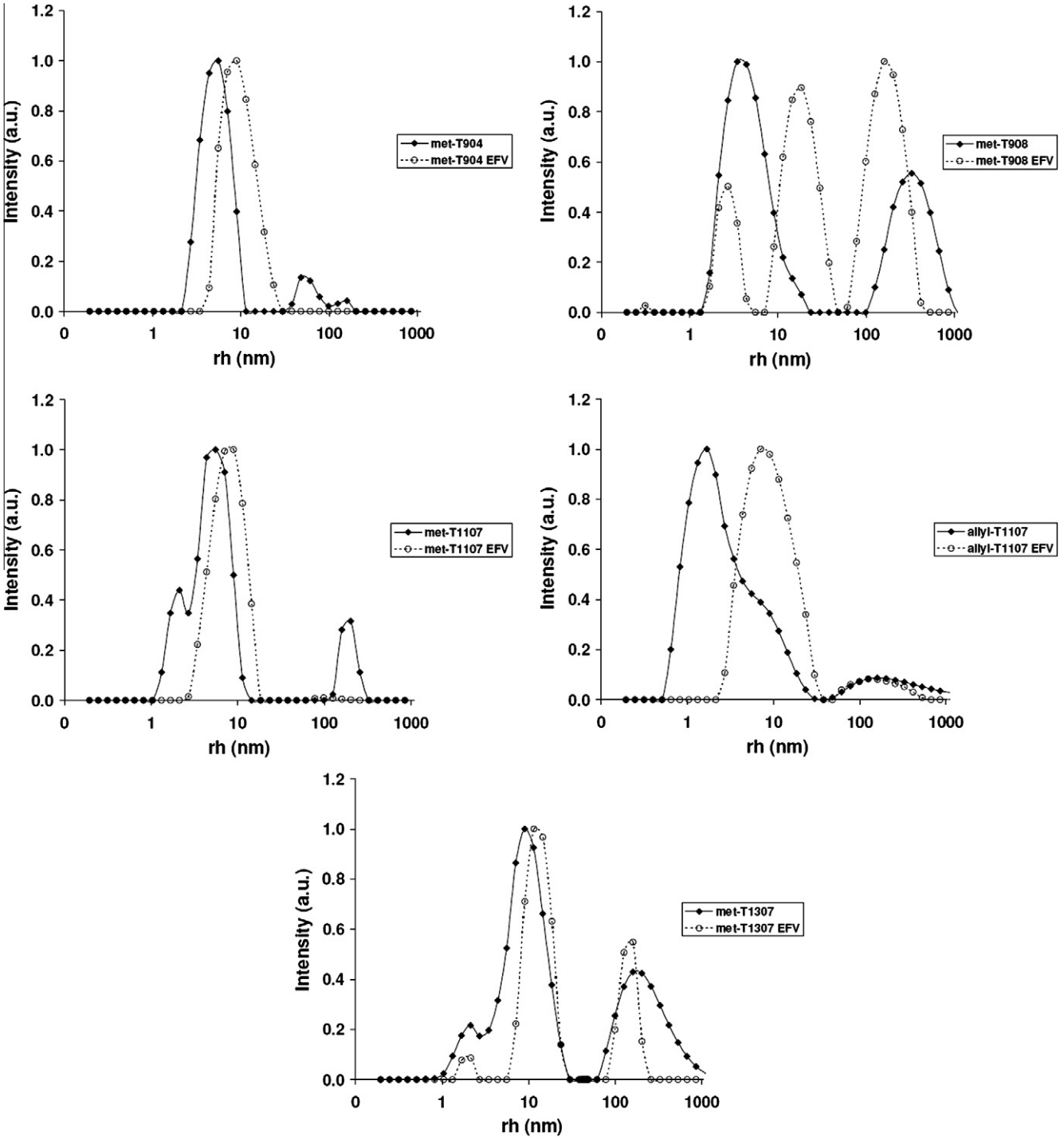

Fig. 9. Hydrodynamic radii and radii distribution of EFV-free and EFV-loaded micelles, as measured by DLS. The polymer concentration is 10%.

micelles under dilution, a faster release was found. A similar trend was found for T1307, the modified copolymer releasing 53.3% versus 33.6% of the pristine one.

These findings suggest that the incorporation of *N*-alkyl groups to the poloxamine structure favors the disassembly of the micelles and weakens the drug/core interaction, without significantly compromising the drug loading capacity.

4. Conclusions

Since recent years, micellar systems have become a key tool toward the improvement of the aqueous solubility and the chemical stability of hydrophobic drugs. Although the contribution of poloxamines to this field has been somehow neglected, in the present work we stressed the potential of these dually responsive molecules and their *N*-alkylated derivatives in the context of modulating the drug solubilization and delivery of EFV, a first-line antiretroviral used in the treatment of HIV toward its oral administration. The aqueous solubility of the drug was increased from 0.004 mg/mL to approximately 30 mg/mL, representing the best solubilization performance in aqueous medium of any nanocarrier described yet. It is also worth remarking that the presence of EFV in the medium promoted the aggregation of the different copolymers. Moreover, the *N*-alkylation (with just a minor structural modification, i.e.,

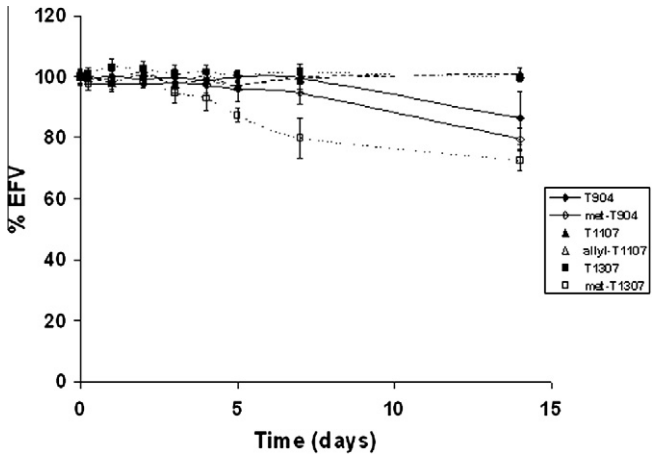

Fig. 10. % EFV in solution of diluted drug-loaded polymeric micelles over time at 37 °C.

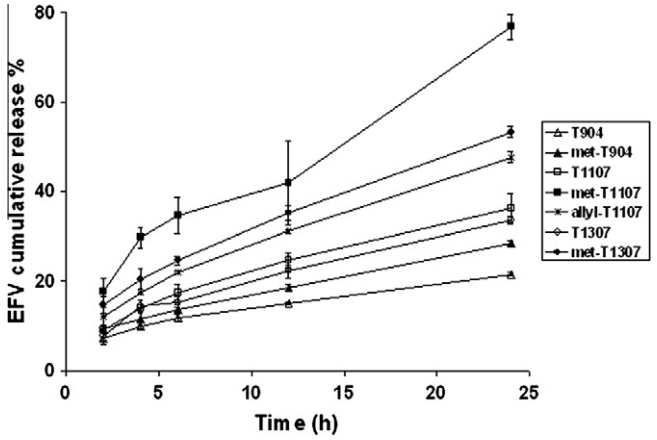

Fig. 11. *In vitro* drug release profiles in PBS (pH 7.4) at 37 °C from 1/10 diluted EFV-containing 10% T904, 10% met-T904, 10% T1107, 10% met-T1107, 10% allyl-T1107, 10% T1307, and met-T1307. Means ± SD of triplicate assays are shown.

Table 6
Results of the fitting of EFV release profiles from pristine and *N*-alkylated poloxamine micelles to zero-order kinetics ($M = k_0 t$).

Copolymer	k_0	R^2
T904	0.615	0.977
Met-T904	0.854	0.998
T1107	1.182	0.976
Met-T1107	2.48	0.972
Allyl-T1107	1.565	0.987
T1307	1.088	0.966
Met-T1307	1.705	0.992

k_0: zero order release constant (%/h).

one methyl- or allyl-group per molecule) enabled to increase the drug release rate from the micellar reservoir *in vitro*. Overall results stress the potential and versatility of poloxamines as micellar carriers physically stable under dilution but that deliver the drug at a modulable rate, and support the implementation of these materials in the development of novel pediatric anti-HIV medicines for oral pharmacotherapy.

Acknowledgements

This work was financed by Agencia Española de Cooperación Internacional para el Desarrollo (AECID Grant A/016343/08, MAE, Spain). The authors express their gratitude to A. Santoveña (Universidad de La Laguna, Spain) for help with GPC analysis and to BASF Corporation (Verena Geiselhart) for providing poloxamine samples.

References

[1] A. Sosnik, A.M. Carcaboso, D.A. Chiappetta, Polymeric nanocarriers: new endeavors for the optimization of the technological aspects of drugs, Recent Pat. Biomed. Eng. 1 (2008) 43–59.
[2] D.A. Chiappetta, A. Sosnik, Poly(ethylene oxide)–poly(propylene oxide) block copolymer micelles as drug delivery agents: improved hydrosolubility, stability and bioavailability of drugs, Eur. J. Pharm. Biopharm. 66 (2007) 303–317.
[3] J. Dong, B.Z. Chowdhry, S.A. Leharne, Surface activity of poloxamines at the interfaces between air–water and hexane–water, Colloids Surf. A 212 (2003) 9–17.
[4] J. Gonzalez-Lopez, C. Alvarez-Lorenzo, P. Taboada, A. Sosnik, I. Sandez-Macho, A. Concheiro, Self-associative behavior and drug-solubilizing ability of poloxamine (Tetronic) block copolymers, Langmuir 24 (2008) 10688–10697.
[5] C. Alvarez-Lorenzo, J. Gonzalez-Lopez, M. Fernandez-Tarrio, I. Sandez-Macho, A. Concheiro, Tetronic micellization, gelation and drug solubilization: influence of pH and ionic strength, Eur. J. Pharm. Biopharm. 66 (2007) 244–252.
[6] D.A. Chiappetta, J. Degrossi, S. Teves, M. D'Aquino, C. Bregni, A. Sosnik, Triclosan-loaded poloxamine micelles for enhanced topical antibacterial activity against biofilm, Eur. J. Pharm. Biopharm. 69 (2008) 535–545.
[7] D.A. Chiappetta, J. Degrossi, R.A. Lizarazo, D.L. Salinas, F. Martínez, A. Sosnik, Molecular implications in the solubilization of the antibacterial agent triclocarban by means of branched poly(ethylene oxide)–poly(propylene oxide) polymeric micelles, in: L. Segewicz, M. Petrowsky (Eds.), Polymer aging, stabilizers and amphiphilic block copolymers, Nova Science Publishers, Hauppauge, 2010, pp. 197–211.
[8] C. Roques, K. Bouchemal, G. Ponchel, Y. Fromes, E. Fattal, Parameters affecting organization and transfection efficiency of amphiphilic copolymers/DNA carriers, J. Control. Release 138 (2009) 71–77.
[9] C. Roques, E. Fattal, Y. Fromes, Comparison of toxicity and transfection efficiency of amphiphilic block copolymers and polycationic polymers in striated muscles, J. Gene Med. 11 (2009) 240–249.
[10] A. Sosnik, M.V. Sefton, Methylation of poloxamine for enhanced cell adhesion, Biomacromolecules 7 (2006) 331–338.
[11] D.A. Chiappetta, C. Hocht, C. Taira, A. Sosnik, Efavirenz-loaded polymeric micelles for pediatric anti-HIV pharmacotherapy with significantly higher oral bioavailaibility, Nanomedicine 5 (2010) 11–23.
[12] A. Sosnik, D.A. Chiappetta, A.M. Carcaboso, Drug delivery systems in HIV pharmacotherapy: what has been done and the challenges standing ahead, J. Control. Release 138 (2009) 2–15.
[13] B. Gazzard, British HIV association (BHIVA) guidelines for the treatment of HIV infected adults with antiretroviral therapy, HIV Med. 7 (2006) 487–496.
[14] U. Wintergerst, F. Hoffmann, A. Jansson, G. Notheis, K. Huss, M. Kurowski, D. Burger, Antiviral efficacy, tolerability and pharmacokinetics of efavirenz in an unselected cohort of HIV-infected children, J. Antimicrob. Chemother. 61 (2008) 1336–1339.
[15] C. Csajka, C. Marzollini, K. Fattinger, L.A. Décosterd, A. Telenti, J. Biollaz, T. Buclin, Population pharmacokinetics and effects of efavirenz in patients with human immunodeficiency virus infection, Clin. Pharm. Ther. 73 (2003) 20–30.
[16] S.M. Bahal, J.M. Romansky, F.J. Alvarez, Medium chain triglycerides as vehicle for palatable oral liquids, Pharm. Dev. Technol. 8 (2003) 111–115.
[17] Y.H. Bae, H. Yin, Stability issues of polymeric micelles, J. Control. Release 131 (2008) 2–4.
[18] S.W. Provencher, Inverse problems in polymer characterization: direct analysis of polydispersity with photon correlation spectroscopy, Makromol. Chem. 180 (1979) 201–209.
[19] M.B. Huglin, Light Scattering from Polymer Solutions, Plenum Press, New York, 1972. pp. 165–331.
[20] E. Gulari, B. Chu, T.Y. Liu, Characterization of meningococcal polysaccharides by light-scattering spectroscopy. IV. Molecular weight distribution of group B meningococcal polysaccharide in buffer solution, Biopolymers 18 (1979) 2943–2961.
[21] H. Altinok, S.K. Nixon, P.A. Gorry, D. Attwood, C. Booth, A. Kelarakis, V. Havredaki, Micellisation and gelation of diblock copolymers of ethylene oxide and propylene oxide in aqueous solution, the effect of P-block length, Colloids Surf. B 16 (1999) 73–91.
[22] T. Mosmann, Rapid colorimetric assay for cellular growth and survival: application to proliferation and cytotoxicity assays, J. Immunol. Methods 65 (1983) 55–63.
[23] W. He, L.F. Fan, Q. Du, B. Xiang, C.L. Li, M. Bai, Y.Z. Chang, D.Y. Cao, Design and *in vitro*/*in vivo* evaluation of multi-layer film coated pellets for omeprazole, Chem. Pharm. Bull. 57 (2009) 122–128.
[24] N. Bicak, B.F. Senkal, Synthesis and polymerization of *N*,*N*-diallyl morpholinium bromide, Eur. Pol. J. 36 (2000) 703–710.
[25] S.M. Moghimi, A.C. Hunter, J.C. Murray, Long-circulating and target-specific nanoparticles: theory to practice, Pharmacol. Rev. 53 (2001) 283–318.

[26] O. Al-Hanbali, N.M. Onwuzo, K.J. Rutt, C.M. Dadswell, S.M. Moghimi, A.C. Hunter, Modification of the Stewart biphasic colorimetric assay for stable and accurate quantitatitive determination of Pluronic and Tetronic block copolymers for application in biological systems, Anal. Biochem. 361 (2007) 287–293.
[27] M.R. Munch, A.P. Gast, Block copolymer adsorption: heads or tails?, Polym Commun. 30 (1989) 324–326.
[28] J. Dong, B.Z. Chowdry, S.A. Leharne, Solubilisation of polyaromatic hydrocarbons in aqueous solutions of poloxamine T803, Colloids Surf. A 246 (2004) 91–98.
[29] P. Alexandridis, V. Athanassiou, S. Fukuda, T.A. Hatton, Surface activity of poly(ethylene oxide)–block–poly(propylene oxide)–block–poly(ethylene oxide) copolymers, Langmuir 10 (1994) 2604–2612.
[30] C. Chaibundit, N.M.P.S. Ricardo, F.M.L.L. Costa, S.G. Yates, C. Booth, Micellization and gelation of mixed copolymers P123 and F127 in aqueous solution, Langmuir 23 (2007) 9229–9236.
[31] H. Altinok, G-E. Yu, S.K. Nixon, P.A. Gorry, D. Attwood, C. Booth, Effect of block architecture on the self-assembly of copolymers of ethylene oxide and propylene oxide in aqueous solution, Langmuir 13 (1997) 5837–5848.
[32] S. Barbosa, M.A. Cheema, P. Taboada, V. Mosquera, Effect of copolymer architecture on the micellization and gelation of aqueous solutions of copolymers of ethylene oxide and styrene oxide, J. Phys. Chem. B 111 (2007) 10920–10928.
[33] E.F. Casassa, Particle scattering factors in Rayleigh scattering, in: J. Brandrup, E.H. Immergut (Eds.), Polymer Handbook, third ed., Wiley, New York, 1989, p. 485.
[34] W.H. Beattie, C. Booth, Table of dissymmetries and correction factors for use in light scattering, J. Phys. Chem. 64 (1960) 696–697.
[35] J.K. Percus, G.J. Yevick, Analysis of classical statistical mechanics by means of collective coordinates, J. Phys. Rev. 110 (1958) 1–13.
[36] A. Vrij, Light scattering of a concentrated multicomponent system of hard spheres in the Percus–Yevick approximation, J. Chem. Phys. 69 (1978) 1742–1747.
[37] N.F. Carnahan, K.E. Starling, Equation of state for nonattracting rigid spheres, J. Chem. Phys. 51 (1969) 635–636.
[38] J. Dong, J. Armstrong, B.Z. Chowdhry, S.A. Leharne, Thermodynamic modelling of the effect of pH upon aggregation transitions in aqueous solutions of the poloxamine, T701, Thermochim. Acta 417 (2004) 201–206.
[39] Z.K. Zhou, B.J. Chu, Light-scattering study on the association behavior of triblock polymers of ethylene oxide and propylene oxide in aqueous solution, Colloid Interface Sci. 126 (1988) 171–180.
[40] A. Sosnik, M.V. Sefton, Semi-synthetic collagen/poloxamine matrices for tissue engineering, Biomaterials 26 (2005) 7425–7435.
[41] A. Sosnik, B. Leung, A.P. McGuigan, M.V. Sefton, Collagen/poloxamine hydrogels: cytocompatibility of embedded HepG2 cells and surface attached endothelial cells, Tissue Eng. 11 (2005) 1807–1816.
[42] A. Sosnik, M.V. Sefton, Poloxamine hydrogels with a quaternary ammonium modification to improve cell attachment, J. Biomed. Mater. Res. 75A (2005) 295–307.
[43] A. Sosnik, B.M. Leung, M.V. Sefton, Lactoyl-poloxamine/collagen matrix for cell-containing modules, J. Biomed. Mater. Res. – A 86 (2008) 339–353.
[44] T. Decker, M.L. Lohmann-Matthes, A quick and simple method for the quantitation of lactate dehydrogenase release in measurements of cellular cytotoxicity and tumor necrosis factor (TNF) activity, J. Immunol. Methods 15 (1988) 61–69.
[45] A.V. Kabanov, E.V. Batrakova, V.Y. Alakhov, Pluronic® block copolymers for overcoming drug resistance in cancer, Adv. Drug Del. Rev. 54 (2002) 759–779.
[46] J. Green, M. Heald, K.H. Baggaley, R.M. Hindley, B. Morgan, Tetronic 701 – a novel hypocholesterolaemic agent, Atherosclerosis 23 (1976) 549–558.
[47] M. Imayasu, A. Shiraishi, Y. Ohashi, S. Shimada, H.D. Cavanagh, Effects of multipurpose solutions on corneal epithelial tight junctions, Eye Contact Lens 34 (2008) 50–55.
[48] M.E. Cavet, K.L. Harrington, K.R. VanDerMeid, K.W. Ward, J.-Z. Zhang, Comparison of the effect of multipurpose contact lens solutions on the viability of cultured corneal epithelial cells, Cont. Lens Anterior Eye 32 (2009) 171–175.
[49] J.S. Palmer, W.J. Cromie, R.C. Lee, Surfactant administration reduces testicular ischemia-reperfusion injury, J. Urol. 159 (1998) 2136–2139.
[50] Medecins sans Frontieres. Press Release. <http://www.msf.org/> (accessed 07.09).
[51] C. Giaquinto, E. Morelli, F. Fregonese, O. Rampon, M. Penazzato, A. de Rossi, R. D'Elia, Current and future antiretroviral treatment options in paediatric HIV infection 1, Clin. Drug Invest. 28 (2008) 375–397.
[52] E. Brown, Antiretroviral Therapy in Children, HIV/AIDS Primary Care Guide, AIDS Education & Training Centers National Resource Center, 2007, p. 419 (Chapter 30).
[53] J.F. Standing, C. Tuleu, Paediatric formulations – getting to the heart of the problem, Int. J. Pharm. 300 (2005) 56–66.
[54] Committee on pediatric AIDS (section on international child health), Increasing antiretroviral drug access for children with HIV infection, Pediatrics 119 (2007) 838–845.
[55] I. Choonara, S. Conroy, Unlicensed and off-label drug use in children: implications for safety, Drug. Saf. 25 (2002) 1–5.
[56] T. Nunn, J. Williams, Formulation of medicines for children, Br. J. Clin. Pharmacol. 59 (2005) 674–676.
[57] T. Eileen Kairuz, D. Gargiulo, C. Bunt, S. Garg, Quality, safety and efficacy in the 'off-label' use of medicines, Curr. Drug Safety 2 (2007) 89–95.
[58] A. Sosnik, D.A. Chiappetta, A. Carcaboso, Drug delivery systems in HIV pharmacotherapy: what has been done and the challenges standing ahead, J. Control Release 138 (2009) 2–15.
[59] A. Sosnik, M. Amiji, Nanotechnology solutions for infectious diseases in developing nations, Adv. Drug Del. Rev. 62 (2010) 375–377.
[60] WHO/Make Medicines Child Size, <http://www.who.int/childmedicines/en/> (accesed 07.09).
[61] S.M. Bahal, J.M. Romansky, F.J. Alvarez, Medium chain triglycerides as vehicle for palatable oral liquids, Pharm. Dev. Technol. 8 (2003) 111–115.
[62] L. Wang, X. Zhang, S. Pooyan, M.S. Palombo, M.J. Leibowitz, S. Stein, P.J. Sinko, Optimizing size and copy number for PEG–fMLF (*N*-formyl-methionyl-leucyl-phenylalanine) nanocarrier uptake by macrophages, Bioconj. Chem. 19 (2008) 28–38.
[63] D.A. Chiappetta, C. Hocht, A. Sosnik, A highly concentrated and taste-improved aqueous formulation of efavirenz for a more appropriate pediatric management of the anti-HIV therapy, Curr. HIV Res. 8 (2010) 23–31.
[64] G. Riess, Micellization of block copolymers, Prog. Polym. Sci. 28 (2003) 1107–1170.
[65] C. Allen, D. Maysinger, A. Eisenberg, Nano-engineering block copolymer aggregates for drug delivery, Colloids Surf. B 16 (1999) 3–27.
[66] R.L. Xu, M.A. Winnik, F.R. Hallett, G. Riess, M.D. Croucher, Light-scattering study of the association behavior of styrene–ethylene oxide block copolymers in aqueous solution, Macromolecules 24 (1991) 87–93.